SEISMIC BEHAVIOUR OF THIN/SLENDER CONCRETE WALLS WITH MONOLITHIC EMULATION BASE CONNECTIONS TESTED ON SHAKING TABLE

(Date received: 23.7.2007)

Nor Hayati Abdul Hamid[1], Lionel Linayage[2] and John B. Mander[3]

[1]Lecturer, PhD, Faculty of Civil Engineering, Universiti Teknologi MARA, 40450 Shah Alam, Selangor

[2]Former Postgraduate Student, University of Canterbury, Christchurch, New Zealand

[3]Professor, Zachry Department of Civil Engineering, Texas A& M University, TX 77843, U.S.A.

Email: abdulhamid_nrhyt@yahoo.com

ABSTRACT

Two geometrically identical slender precast concrete walls with monolithic emulation base connections were constructed and tested under biaxial loading using two clover displacement control patterns on shaking table. Specimen 1 was constructed with 1.27% longitudinal reinforcement bars which exceeding the requirement in BS 8110 and NZ 3101 while Specimen 2 was 0.54% longitudinal reinforcement bars within the range specified in BS 8110 and NZ 3101. Both specimens were subjected to quasi-static bilateral loading which was supplied by hydraulic double actuator. In-plane and out-of-plane drifts were applied to both specimens using Lissajous functions. Specimen 1 was subjected to 0.5%, 1.0% and 1.5% drift within two cycles in each drift. This wall failed in lateral torsional buckling mechanism with ductility of 3. Specimen 2 was tested at 0.5%, 1.0%, 1.5% and 2.0% drift. This specimen started to crack at 0.5% and more cracks were observed at 1.0% drift. This wall failed by low cycle fatigue behaviour associated with compression failure at the bottom of the wall with ductility of 4. It can be concluded that even though the slenderness ratio (height/thickness) is limited to 30 but experimental result showed that slenderness ratio 60:1 is still stable under biaxial loading. Experimental results showed that an increase of longitudinal reinforcement did not attribute to better seismic performance of thin/slender precast wall panels.

Key words: *Metal Injection Molding (MIM), Optimisation, Pareto-Anova, Taguchi, S/N Ratio*

1.0 INTRODUCTION

In monolithic construction the inelastic response of a wall during seismic events is restricted by deformations of plastic hinge zones that form at the base of the wall. Recently, the structural engineers tend to design very thin/slender precast concrete walls for material saving and ease of handling. The slenderness ratio exceeding 60:1 is presently in vogue with the thickness rarely exceeding 150mm which normally used in the construction of warehouse buildings. These walls commonly possess only a single central layer of reinforcement or fabric wire mesh which provides sufficient strength while maintaining the codes specified minimum concrete cover requirements. This construction practice is contrast with current design codes such as BS 8110 [1], NZS 3101[2] and ACI 318[3] which specify the slenderness ratio should be limited to 30:1 for non-seismic design and 25:1 for seismic design. These provisions may be exceeded if it can be demonstrated by analysis or tests that the walls are stable. It appears that there is no straightforward analysis to confirm the safety and stability of the thin/slender walls. Therefore, it is surprising that the Malaysian, Indonesian, New Zealander and others designers take liberty to exceed the standard limit with significant margins without conducting proof-of-concept tests. It is conceivable that thin wall structure with earthquake induced damage could result in incipient collapse, demolition and rebuilding of the structure would be required after ground shaking.

Precast concrete walls in warehouse buildings are expected to provide a dual function of external cladding and load bearing wall. The wall is designed to carry roof and lateral loading which comes from wind and/or seismic loading as in shown in Figure 1. Previous paper [4] studied on the dynamic response of slender/thin precast wall panels subjected to past earthquake excitation such as Taft, El Centro and Kobe Earthquake using shaking table. It is also important to study the seismic behaviour of this wall panels at slow motion using shaking table under biaxial loading. Hence, this paper is to conduct experimental work on two geometrically identical thin/slender precast wall panels with slenderness ratio of 60:1 using monolithic emulation connections subjected to " 2-clover displacement pattern" which can be categorised as biaxial loading.

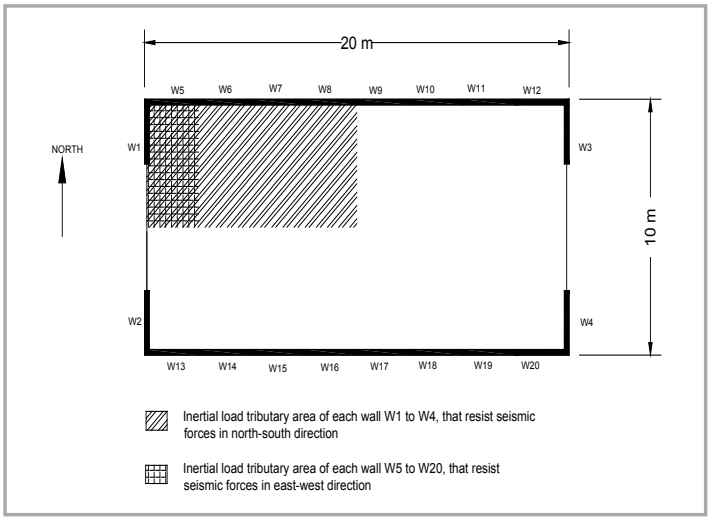

Figure 1: Idealised plan view of warehouse building (20m x 10m)

2.0 EXPERIMENTAL STUDY

The quasi-static biaxial lateral loading tests were conducted on two test specimens with different reinforcement proportions. The specimens were designed based on the information collected from the industry and through the aforementioned literature survey on typical thin precast concrete wall panels that are used in the construction of industrial/warehouse buildings in Malaysia and New Zealand. The seismic performance of the critical walls of this building in particular is the main focus of this study. The critical wall panels are W1 to W4 as shown in Figure 1 which carries very high inertial loads in north-south direction. The prototype wall panels are taken as 125 mm thick, 2400 mm long and 7500 mm high, reinforcement with DH-16 vertical and horizontal rebars. Longitudinal reinforcement was provided in the test specimens to achieve volumetric reinforcement ratios of 1.27% in Specimen 1, and 0.54% in Specimen 2. Details of the walls are identical (except for concrete strengths) to those tested by Sudarno [5]. Monolithic emulative (grouted) base connection was employed for both specimens but the location of the connection was different. The connection in Specimen 1 was provided with longitudinal reinforcement protruding from wall into the base while connection in Specimen 2 was provided with starter bars projecting out from the base block to wall panel. Figure 2 shows the detail dimensions, transverse and longitudinal arrangement of reinforcement bars together with their connections of Specimens 1 and 2.

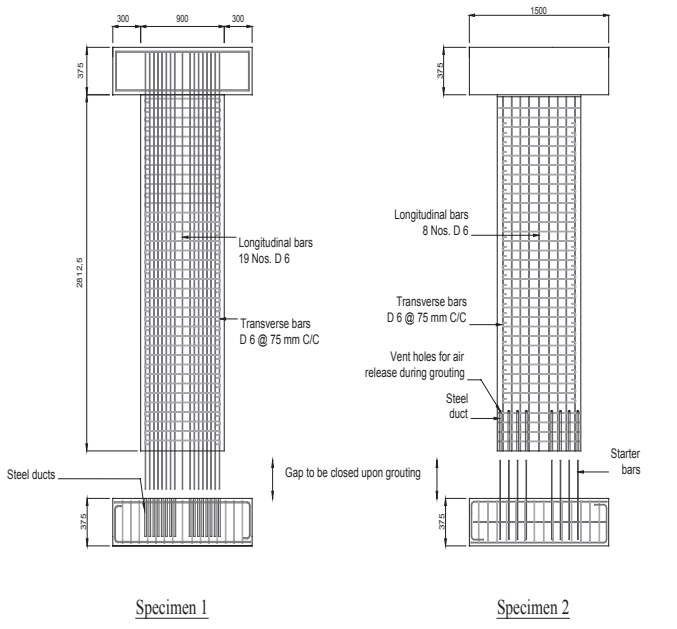

Figure 2: Reinforcement details of Specimend 1 and 2

2.1 SPECIMEN MODELLING

The model to prototype scale factor for the two test specimens was 3/8. The specimen dimensions were 47 mm thick, 900 mm wide and 2810 mm high. Accordingly, 6mm diameter rebars were used in the specimens. Based on the 3/8 length scale adopted for the physical modelling, the following relationships between the prototype and the specimen properties can be established.

Geometric ratio	$Lm/Lp = \lambda = 0.375$
Area ratio	$Am/Ap = \lambda^2$
Force ratio	$Fm/Fp = \lambda^2$
Moment ratio	$Mm/Mp = \lambda^3$

The constant stress and strain similitudes were adopted in the modelling as follows;

$$\sigma_m/\sigma_p = \sigma_m/\sigma_p = 1$$

The subscripts m and p in the above relationships stand for the model properties and the prototype properties respectively. Grade 300 reinforcement was used throughout in the walls. The D6 reinforcement had measured yield strength of f_y = 350 MPa. Concrete with 10mm maximum aggregate size and a specified 28-day compressive strength of 30 MPa was supplied by a ready-mix concrete supplier for both specimens. Slump values of 50 mm and 140 mm were measured for Specimens 1 and 2, respectively. These mixes resulted in 32MPa and 28 MPa measured for strengths at the time of testing.

2.2 CONSTRUCTION OF SPECIMEN 1

Specimen 1 was provided with a longitudinal (vertical) volumetric reinforcement ratio of 1.27%. This ratio slightly exceeds the upper bound limit of 1% in NZ 3101 [2] and enormously exceeds 0.4% in BS8110 [1]. The longitudinal reinforcement used was D6-45 centres. This would translate into D16-120 (Grade 300) or D16-200 (Grade 500) in the prototype. D6-75 centres were used for transverse (horizontal) reinforcement. This translates into D16-200 (Grade 300) or D16-333 (Grade 500) in the prototype. The specimen was cast horizontally on a strong back as shown in Figure 3 that provided stiffness to the specimen during handling and allowed to remain intact until the specimen was erected in its final position for testing. The specimen was cast together with a monolithic concrete block at one end and with the longitudinal reinforcement protruding at the other end over a length of 300 mm (equivalent to fifty times the rebar diameter) sufficient for the development of anchorage bond.

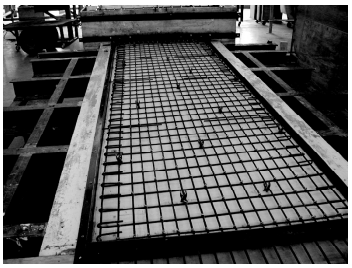

(a) Singly reinforcement bars in wall panel

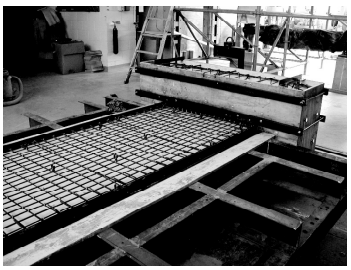

(b) Wall and monolithic-block ready for casting

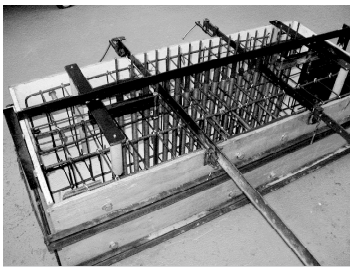

(c) Reinforcement detail of foundation beam

Figure 3: Detailing and construction of Specimen 1

The base blocks were made deliberately large and designed to remain elastic during testing precluding any plastic deformation propagating from the wall panels. HD10 and D6 rebars were used respectively for longitudinal and transverse reinforcement in the base blocks. The base block was cast simultaneously but separate from the wall with provisions for a grouted-connection to the wall. Steel corrugated ducts of 22mm internal diameter were provided within the base block to accommodate longitudinal rebars protruding from the wall and the grout. This arrangement, was different to the common practice where the ducts are provided within the wall, however was necessary given the large number of ducts that had to be accommodated. The monolithic concrete block at the top of wall was identical in size and reinforcement to the base block. This block together with another concrete block of size 1500 mm x 650 mm x 225 mm was designed to provide the simulated stress due to gravity at the bottom of the wall during testing.

2.3 CONSTRUCTION OF SPECIMEN 2

Specimen 2 was provided with longitudinal (vertical) volumetric reinforcement ratio of 0.54%. This reinforcement ratio is well within the NZS 3101 [2] code specified range of 0.2% to 1% and close 0.4% in BS 8110 [1]. Most of the other aspects of construction including the grouted-connection arrangement were kept as close as possible to those used in industry. The corrugated steel ducts for grouted-connection were provided within the wall as shown in Figure 4 and the steel starter bars were provided projecting out from the base block. The grouting was done with a flowing mix of grout (SIKA 215) and was gravity-fed to each individual duct separately while the wall was kept at a slight angle to the horizontal position. The gap between the wall and the base block was filled with a more stiff mix of the same grout material and allowed to dry before commencing grouting of the ducts. Vent holes provided at the upper ends of the ducts ensured the liberation of air from the ducts during grouting. Seven-day compressive strength values of over 40MPa were measured in the compressive strength tests on grout.

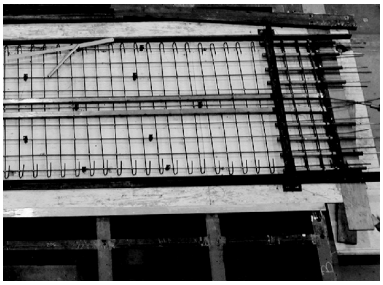

(a) Detail reinforcement bars in wall

(b) View showing the grout ducts at the base of the wall

Figure 4: Detail and construction of Specimen 2

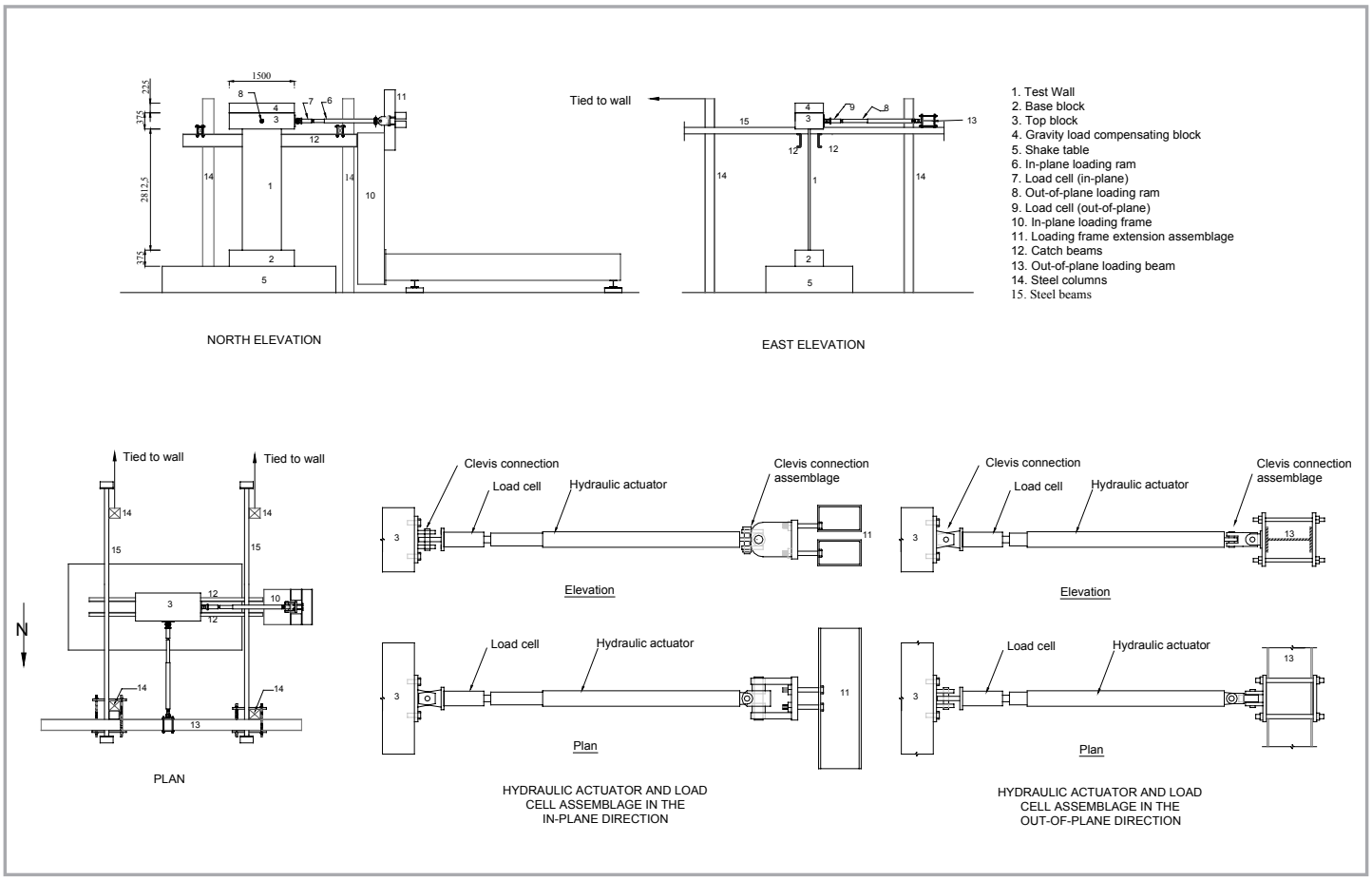

Figure 5: Details of experimental setup

3.0 EXPERIMENTAL SETUP

The shaking table was used to apply quasi-static in-plane drifts (in east-west direction) at the bottom of the specimen while the top of the specimen was restrained in-plane direction. A hydraulic actuator was connected at top of the specimen in-plane direction only to monitor and to make real-time adjustments through a manually operated oil pump to counter any in-plane movement of the specimen. The out-of-plane drift (in north-south direction) was applied simultaneously by means of a hydraulic actuator connected at the top of the specimen.

Figure 5 shows the details of experimental set-up for thin wall seated on shaking table. The reaction frame for in-plane loading consisted of an extended steel column that was attached to the laboratory strong floor. A 120 kN capacity hydraulic actuator was bolted to the top of this reaction frame to measure the reactive force; the actuator was allowed to rotate in both horizontal and vertical planes through an assemblage of two pin-joints (Clevis connections).

The reaction frame for out-of-plane loading consisted of four steel columns each bolted down to the strong-floor, braced in the direction of loading by two steel beams, and a third steel beam of substantial section spanning between the two bracing beams. The actuator was fixed to the latter member through an assemblage of two pin-joints allowing rotation in both horizontal and vertical planes. The capacity and the stroke of the actuator were similar to those of the in-plane actuator, but a 50kN load-cell was used in this direction. The actuator/load-cell assembly was connected to the specimen through a pin-joint in the vertical plane.

Figure 6 shows the photograph of experimental set-up for slender wall which was ready to test for in-plane and out-of-plane loading. The specimen was fixed to the shaking table so that both horizontal and vertical movements of the specimen with respect to shaking table were restrained at the bottom. An additional 500kg concrete block was fixed on the top concrete block to simulate the gravity stresses at the bottom of the specimen. Two more steel beams were fixed from beneath, and spanning in the in-plane direction between, the two bracing beams. These beams were, fixed about 200mm away from the faces of the wall, to provide lateral stability to the out-of-plane loading frame and also to catch the top concrete block in the event of a collapse of the specimen after failure of the specimen.

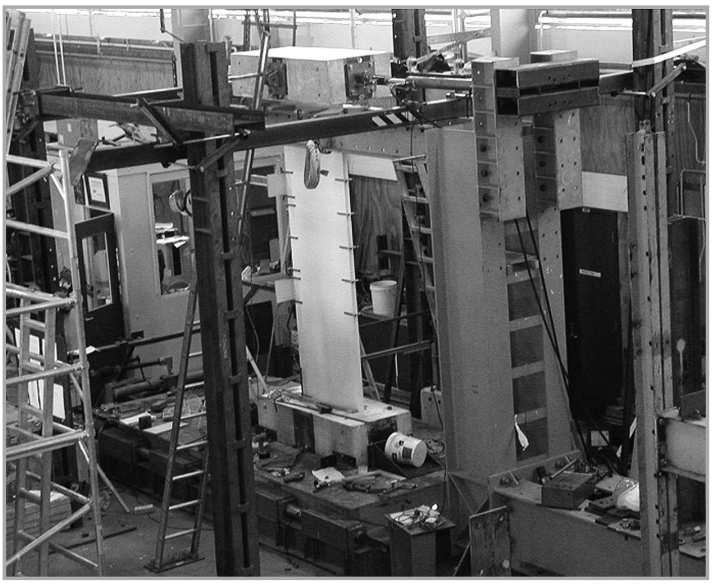

Figure 6: A photograph of experimental setup for thin wall

Figure 7 shows the target biaxial displacement and time histories which were imposed to the wall panel. Biaxial quasi-static reversed cycle lateral loading was applied simultaneously on both principal orthogonal directions with the drifts in both directions changed in a pattern determined according to Bowditch (sometimes referred to as Lissajous) functions. Accordingly, the in-plane and out-of-plane drifts θ_{in} and θ_{oop} were controlled in the time domain as follows.

$$\theta_{in} = (\theta_0)_{in} \sin(2\theta f_{in} t) \quad (1)$$

$$\theta_{oop} = (\theta_0)_{oop} \sin(2\theta f_{oop} t + \theta) \quad (2)$$

where (θ_0)in and (θ_0)oop are the in-plane and out-of-plane drift amplitudes; f_{in} and f_{oop} are the in-plane and out-of-plane frequencies of loading; θ the phase angle; and t the time.

The Bowditch functions have previously been used for drift control in the case of biaxial loading testing on a wall type bridge pier by Estevez [6] whose loading path is similar as target biaxial displacement in Figure 7 with a out-of-plane to in-plane frequency ratio of 0.34. In this study, the frequency ratio was set at 0.4 for the initial test on Specimen 1 and frequency ratio was set to 2 for Specimen 2.

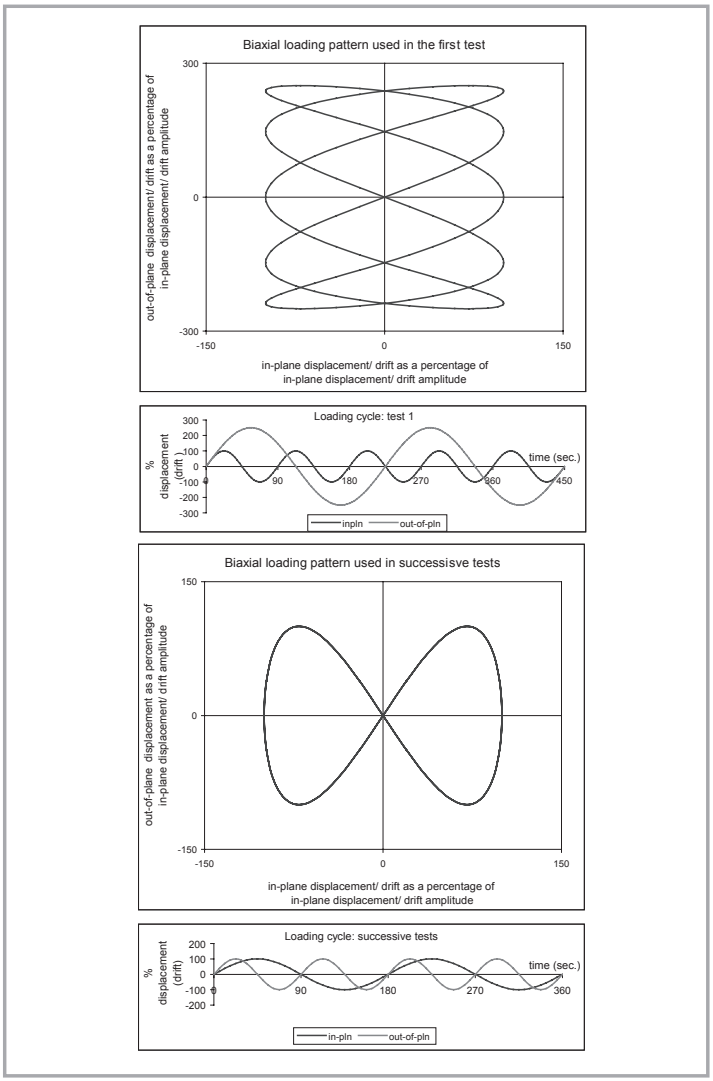

*Displacements and/or drifts are plotted as a percentage of in-plane amplitude of displacement and/or drift in the time history plots.

Figure 7: Target biaxial displacement paths and time histories.

Figure 8 shows the locations of in-plane and out-of-plane potentiometers on thin precast wall panel seated on shaking table. The instrumentation consisted of load-cells for measuring in-plane and out-of-plane lateral forces, and 27 potentiometer/ displacement transducers for measuring in-plane and out-of-plane displacements at different positions along the height of the specimen. The locations of the load cells are shown in Figure 5 and the locations of potentiometers are shown in Figure 8.

Data was signal conditioned and logged unto a purpose-built data logger. Several channels of data such as Channels 16, 26, and 27 were observed in real time during the execution of experiments. Following each test, the logged data was archived for subsequent data processing. Both specimens were tested on shaking table to measure the in-plane and out-of-plane loading subjected to 'two-leaf clover' patterns with displacement control.

4.0 EXPERIMENTAL RESULTS

During experimental work, both specimens were oriented in-plane direction by lying in the east-west direction. Therefore, the notation of test E-W indicated in-plane direction and N-S denoted as out-of-plane direction. For example, if the notation was written as 0.25%(E-W)/0.625%(N-S) means that a test with in-plane and out-of-plane drift amplitudes set at 0.25% and 0.625% respectively. The characteristic of biaxial drift cycles for Specimen 1 is shown in Table 1 and for Specimen 2 is shown in Table 2. Figure 9 shows the complete histories of loading for both specimens by giving both the actual displacement paths and time histories for all the loading cycles.

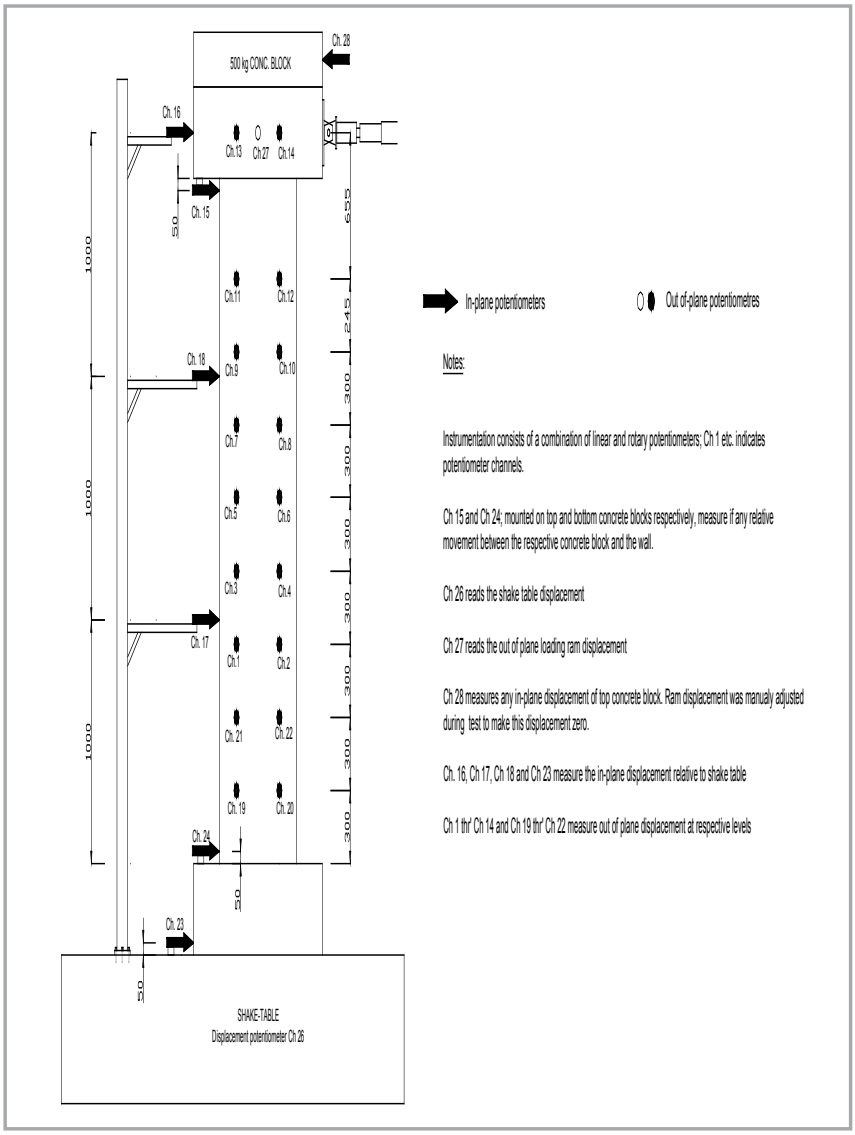

Figure 8: Displacement measurement location

Table 1: Characteristic of biaxial drift cycles, Specimen 1

	TEST	NUMBER OF DRIFT CYCLES		DRIFT (%)		FREQUENCY & (PERIOD)	
		E-W	N-S	E-W	N-S	E-W	N-S
1	0.25 % (E-W) / 0.625 % (N-S	5	2	0.25	0.625	0.011Hz (90sec.)	0.0044Hz (225sec.)
2	0.25 % (E-W) / 0.25 % (N-S)-1	1	2	0.25	0.25	0.0028Hz (360sec.)	0.0056Hz (180sec.)
3	0.25 % (E-W) / 0.25 % (N-S)-2	1	2	0.25	0.25	0.0022Hz (450sec.)	0.0044Hz (225sec.)
4	0.25 % (E-W) / 0.25 % (N-S)-3	2	4	0.25	0.25	0.0022Hz (450sec.)	0.0044Hz (225sec.)
5	0.25 % (E-W) / 0.25 % (N-S)-4	2	4	0.25	0.25	0.0014Hz (720sec.)	0.0028Hz (360 sec)
6	0.25 % (E-W) / 0.25 % (N-S)-5	1	2	0.25	0.25	0.0014Hz (720sec.)	0.0028Hz (360 sec)
7	0.5 % (E-W) / 0.5 % (N-S)-1	-	1	0.5	0.5	0.0014Hz (720sec.)	0.0028Hz (360 sec)
8	0.5 % (E-W) / 0.5 % (N-S)-2	-	1	0.5	0.5	0.0014Hz (720sec.)	0.0028Hz (360 sec)
9	0.5 % (E-W) / 0.5 % (N-S-3	1	2	0.5	0.5	0.0014Hz (720sec.)	0.0028Hz (360 sec)
10	1.0 % (E-W) / 1.0 % (N-S)-1	1	2	1.0	1.0	0.0007Hz (1440sec.)	0.0014Hz (720sec.)
11	1.0 % (E-W) / 1.0 % (N-S)-2	1	2	1.0	1.0	0.0007Hz (1440sec.)	0.0014Hz (720sec.)
12	1.5 % (E-W) / 1.5 % (N-S)	-	1	1.5	1.5	0.0007Hz (1440sec.)	0.0014Hz (720sec.)

Table 2: Characteristics of biaxial drift cycles, Specimen 2

	TEST	NUMBER OF DRIFT CYCLES		DRIFT (%)		FREQUENCY & (PERIOD)	
		E-W	N-S	E-W	N-S	E-W	N-S
1	0.25 % (E-W) / 0.25 % (N-S)	2	4	0.25	0.25	0.0014 Hz (720 sec.)	0.0028 Hz (360 sec.)
2	0.5 % (E-W) / 0.5 % (N-S)	2	4	0.5	0.5	0.0014 Hz (720 sec.)	0.0028 Hz (360 sec.)
3	1.0 % (E-W) / 1.0 % (N-S)-sp1	1/2	3	1.0	1.0	0.0014 Hz (720 sec.)	0.0028 Hz (360 sec.)
4	1.0 % (E-W) / 1.0 % (N-S)	2	4	1.0	1.0	0.0007 Hz (1440 sec.)	0.0014 Hz (720 sec.)
5	1.5 % (E-W) / 1.5 % (N-S)	2	4	1.5	1.5	0.0007 Hz (1440 sec.)	0.0014 Hz (720 sec.)
6	2.0 % (E-W) / 2.0 % (N-S)	1	2	2.0	2.0	0.0007 Hz (1440 sec.)	0.0014 Hz (720 sec.)

The out-of-plane loading was done at three constant in-plane drifts only. One out-of-plane loading cycle to ±1.0% maximum drift was completed while keeping in-plane drift constant at 0%, 0.33% and 0.67%, then loaded to 1.0% in-plane drift and unloaded without any out-of-plane loading. The in-plane loading was done in the pull direction only.

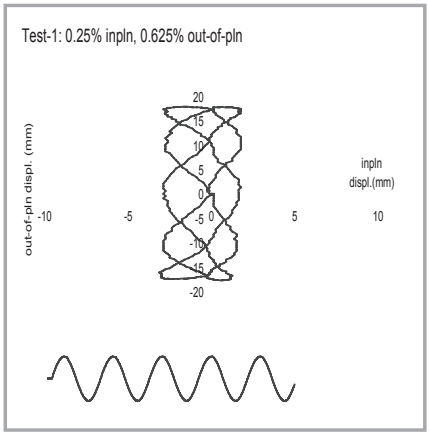

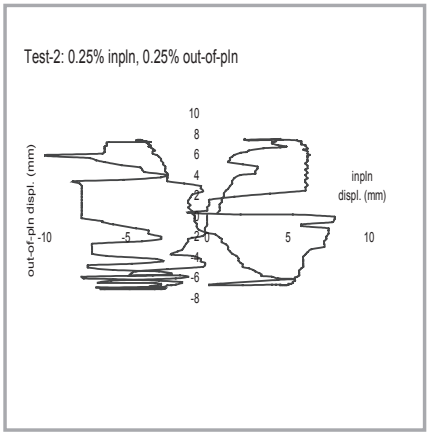

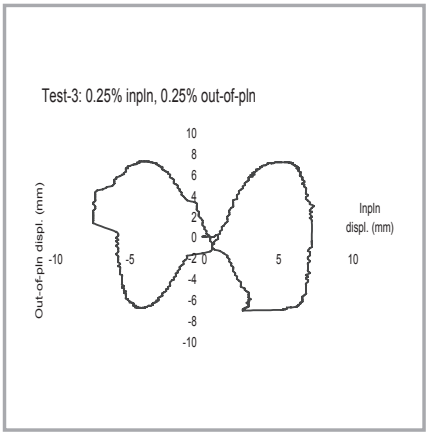

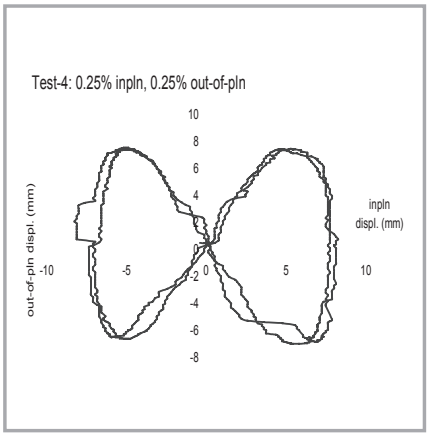

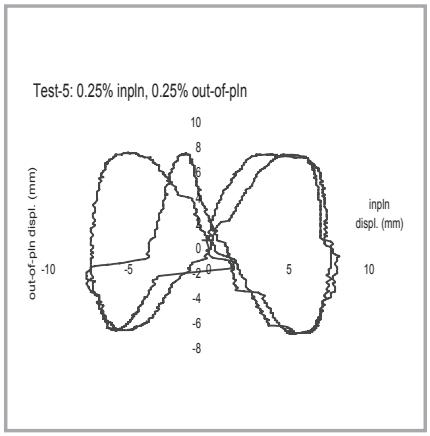

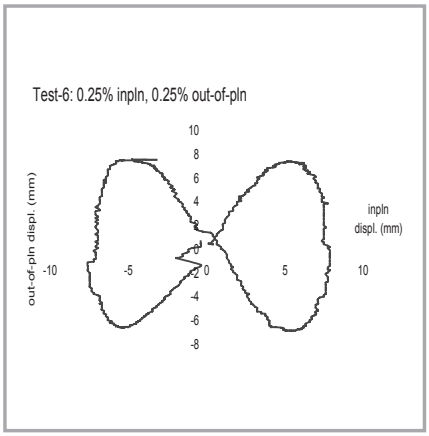

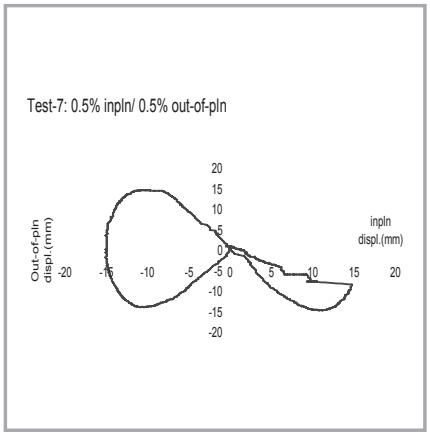

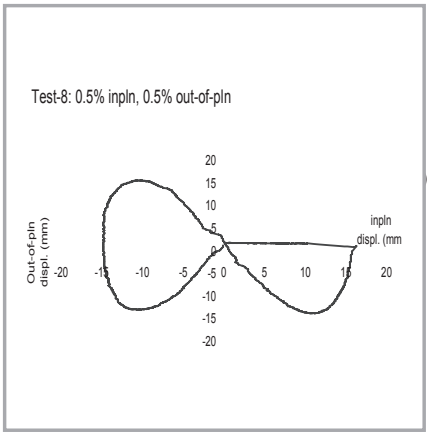

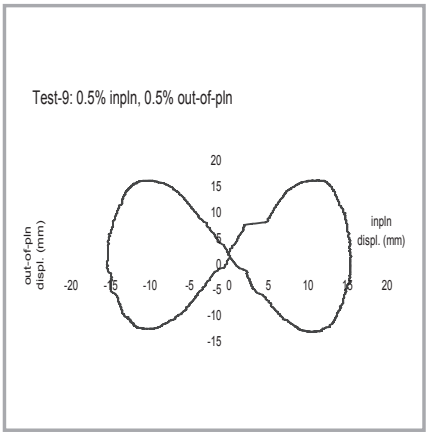

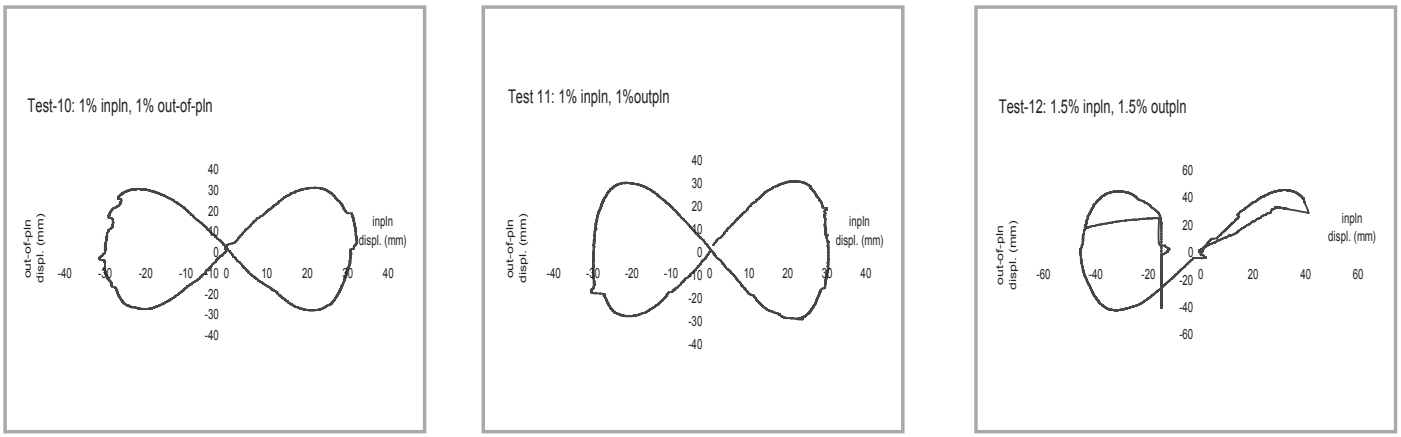

(a) Loading History for Specimen 1

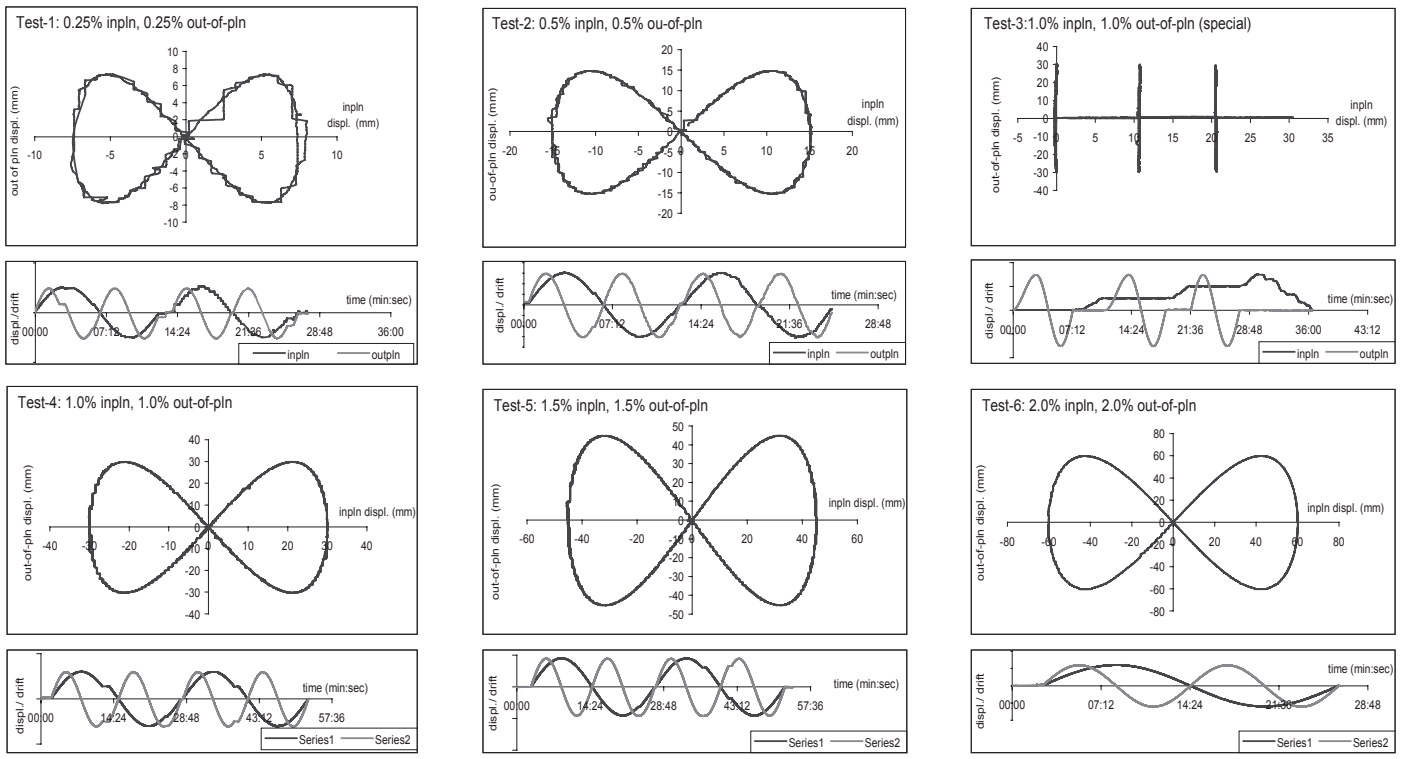

(b) Loading History for Specimen 2

Figure 9: Actual biaxial displacement paths and time histories

4.1 VISUAL OBSERVATION: SPECIMEN 1

The initial testing of Specimen 1 began with 0.25%(E-W)/0.625%(N-S) cycle. The out-of-plane frequency to in-plane frequency ratio was set at 0.4. The specimen was subjected to 5 cycles of 0.25% drift amplitude in-plane direction and 2 cycles of 0.625% drift amplitude out-of-plane direction. Although two lines of horizontal cracks were visible in the lower third of the wall on north-face during the test, the wall response was elastic and no residual out-of-plane displacement could be measured and the cracks closed leaving only hairlines upon unloading. By plotting the displacement history of this test it could be revealed that the actual in-plane displacement amplitude experienced by the wall was significantly smaller than the targeted amplitude of 7.5mm. This resulted from unexpected movements of the in-plane reaction frame. The reaction frame movement was counterbalanced in the subsequent tests by real-time adjustments of in-plane actuator by manual operation of the taps of the oil pump.

Subsequently, a series of loading cycles at 0.25% (E-W)/ 0.25% (N-S) level was carried out at reduced frequency levels until satisfactory manual adjustment of the in-plane displacement could be achieved. The loading cycles were made equi-amplitude (0.25% drift) in both principal orthogonal directions but the out-of-plane to in-plane frequency ratio was set at 2. The respective frequency values of each of the subsequent tests are given in Table 1. Some more horizontal cracking was observed in the lower third of the wall due to out-of-pane displacements during these loading cycles, but the cracks closed upon unloading and only hairlines were visible. No significant residual out-of-plane displacements could be measured.

Figure 10 shows the visual observation on Specimen 1 when subjected to 0.5%, 1.0% and 1.5% drift with two cycles in each drift. There was some instability and vibration in the system during 0.5% (E-W)/0.5 %(N-S)-1, the first loading cycle to 0.5% drift (see Figure 10(a)). Reversing the direction of loading however

was successful and a complete drift envelope at the 0.5% drift amplitude level could be achieved. Horizontal cracking of the wall propagated up to a height of about 1800mm. Some vertical or near-vertical cracks also commenced in the lower 500 mm of the wall. Apparent yielding of some longitudinal reinforcement was also witnessed by the cracking that did not close upon unloading at the base connection.

The cracking of the wall propagated up to a height of about 2000mm during the 1.0% drift cycles [see Figure 10(b)]. A higher proportion of new cracks appeared on the south-face of the wall than on the north-face. Vertical or near-vertical cracks at the bottom part of the wall were observed propagating further up the height of wall. The crack along the wall-to-base connection widened and significant residual out of plane displacements could be observed along the height of the wall.

During 1.5% amplitude drift cycle, the wall suffered initial buckling due to out-of-plane torsion [see Figure 10(c)]. This is during unloading in the out-of-plane direction after reaching the maximum out-of-plane displacement point but before the wall experience maximum displacement in the in-plane direction [see Figure 10(d)]. This buckling was sudden and the wall cracked almost everywhere. The wall then unloaded with respect to both in-plane and out-of-plane directions and loaded in the reverse direction. The wall just survived the 1.5% drift with maximum out-of-plane directions and collapsed by lateral torsional buckling at 1.5% drift at in-plane direction with pushing force [see Figure 10(e)].

4.2 Visual Observation: Specimen 2

A similar test was conducted on Specimen 2 based on Specimen 1. Figure 11 shows the visual observation on Specimen 2 during testing. A significant cracking on Specimen 2 to a height of about 600mm was observed during the first cycle of 0.5% drift level but these cracks closed upon unloading [see Figure 11(a)]. Cracking propagated further up to a height of about 900mm during the second cycle of 0.5% drift. A residual out-of-plane buckling of about 8mm could be measured in the mid-height of the wall.

The specimen was first subjected to one out-of-plane cycle of 1.0% drift amplitude with 0% in-plane drift, then the in-plane drift was increased to 10mm (0.33% drift) and the second out-of-plane cycle of 1.0% drift amplitude was applied. It was observed that the crack along the grout layer at the bottom of the wall has widened and has propagated over the full width of the wall after the 1.0% drift cycles [see Figure 11(b)]. The wall was then subjected to two biaxial cycles of 1.5% drift amplitude. The two outer most reinforcement bars fractured during this test; the grout and the concrete at the base of the wall failed in compression [see Figure 11(d)]. Crushing and spalling off of concrete at the toe regions of the wall could also be observed. One cycle at 2% amplitude drift level was also completed, but due to the fracture of three more bars and crushing of concrete and grout at the base of the wall, no further testing was conducted [see Figure 11(c)].

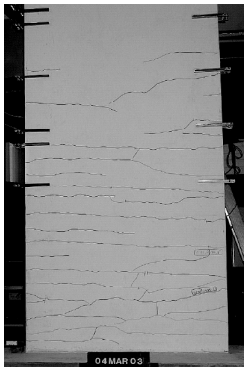

(a) North-face after 0.5% cycles

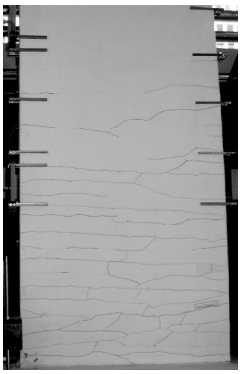

(b) North-face after 1.0% cycles

(c) North-face after failure (1.5% cycle)

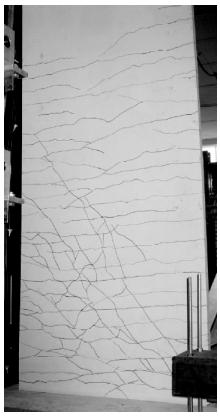

(d) South-face after failure (1.5% cycle)

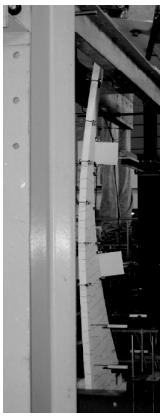

(e) Lateral-torsional buckling failure

Figure 10: Visual observations for Specimen 1

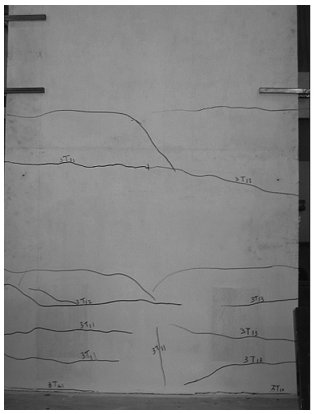

(a) North-face after 0.5% cycles

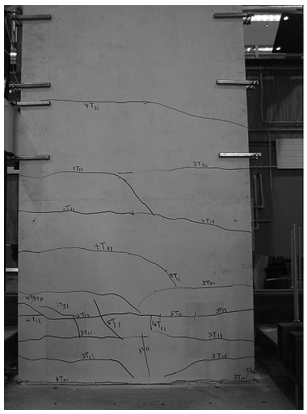

(b) North-face after 1.0% cycle

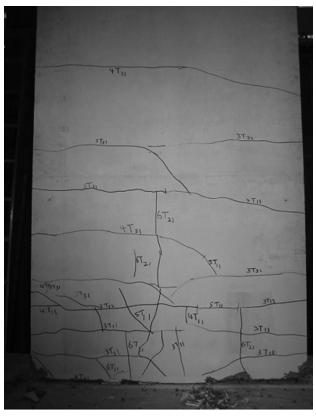

(c) North-face after failure at 2.0%

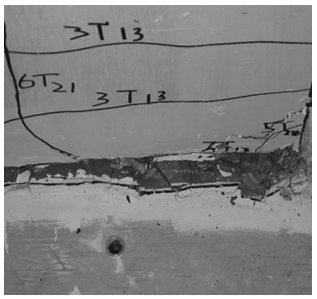

(d) Compression failure of base joint

Figure 11: Visual observations for Specimen 2

5.0 HYSTERETIC RESPONSE

Figure 12 presents the observed lateral load verses displacement performance for each specimen in both in-plane and out-of-plane directions. Also plotted on these graphs are theoretical monotonic pushover curves based on the measured material properties. The theoretical development pushover curves are well explained in Hamid [7]. The response of Specimen 1 appears banded by a bilinear envelope until incipient failure resulting from buckling commenced. However, it will be noted that Specimen 2 showed an in-plane shortfall of strength; this is attributed to weakening induced by the out-of-plane motion. Later a significant loss in strength can be observed in Specimen 2 due to fracture of the starter bars arising from low cycle fatigue effects.

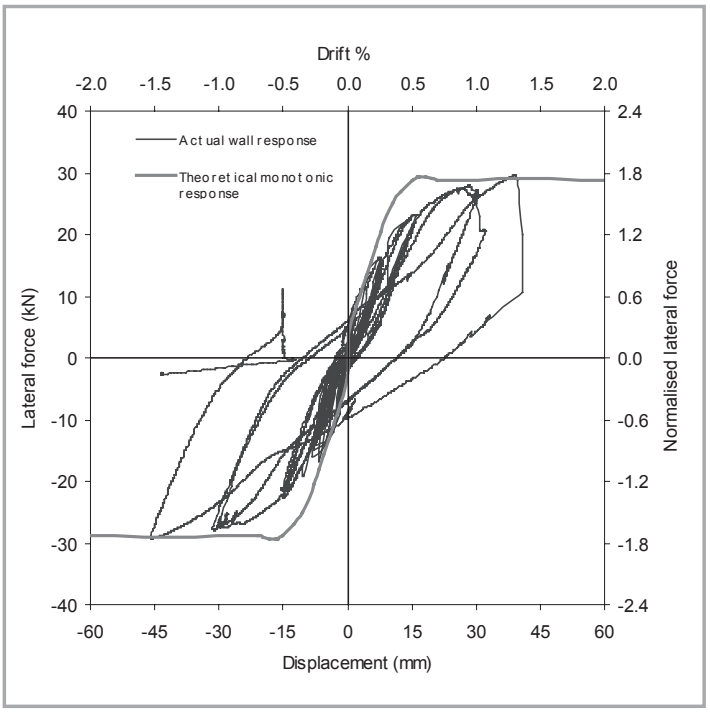

In-plane response Specimen

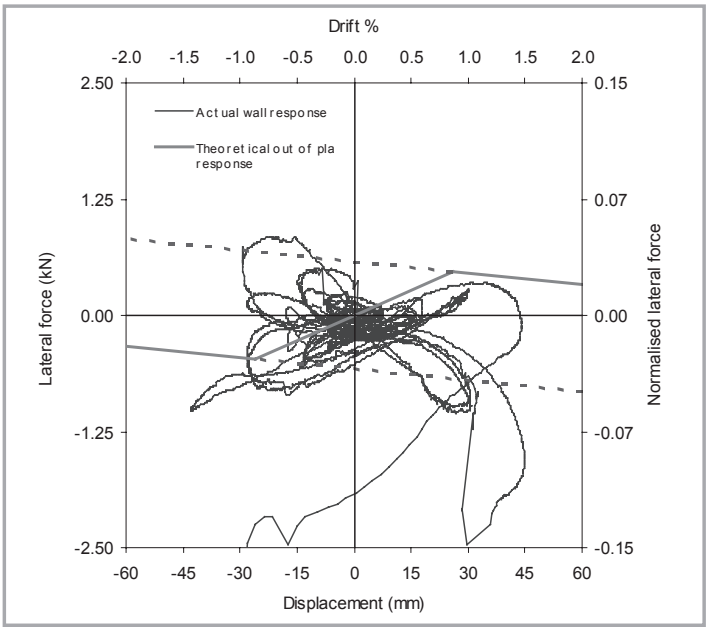

Out-of-plane response Specimen 1

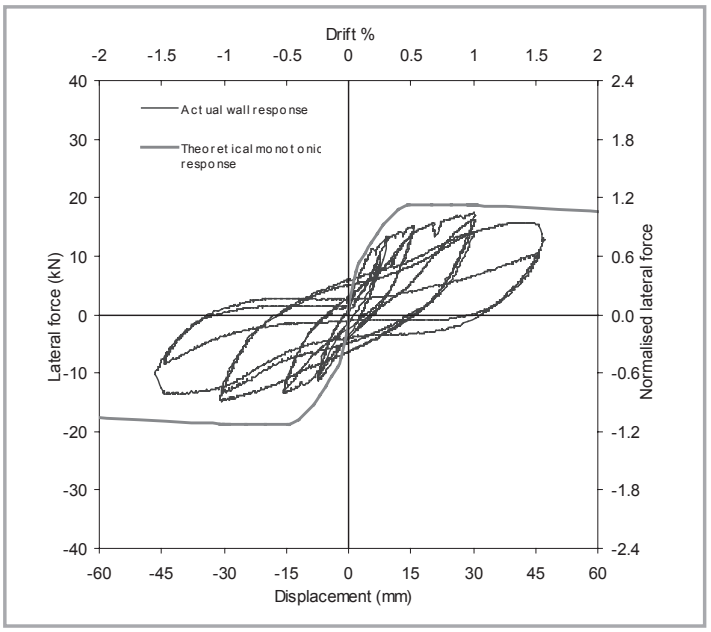

In-plane response Specimen 2

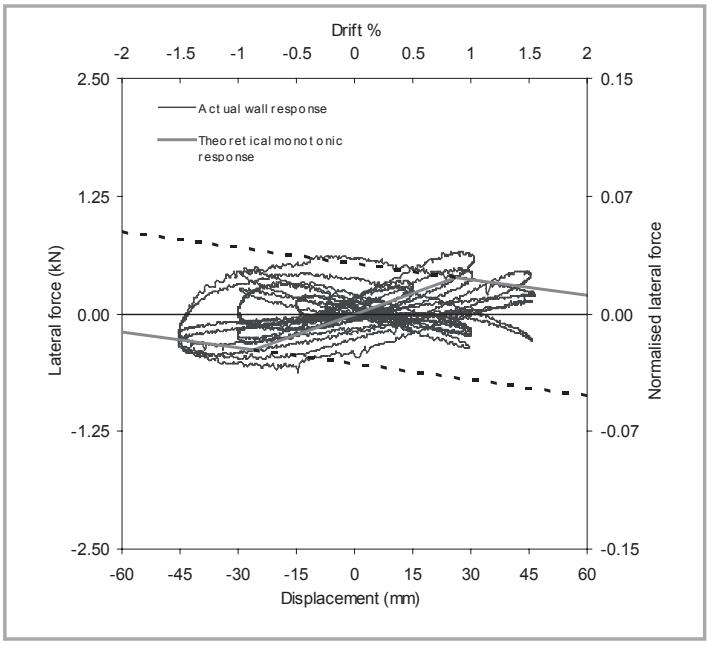

Out-of-plane response Specimen 2

Figure 12: Force verses displacement hysteretic behaviour of the walls

6.0 FAILURE MODES

Specimen 1 failed due to lateral-torsional out-of-plane buckling. The commencement of the buckling occurred at a drift of 1.15% during the 1.5% drift cycle. Prior to this state Specimen 1 did not show adverse buckling performance as evident during the cycle of loading to 1.0% drift cycle as can be seen in Figure 13. However on the final 1.5% drift amplitude incipient buckling occurred. An out-of-plane differential bulge of 70 mm at mid height of the compression end of the wall occurred following the peak in-plane maximum force. On unloading during the in-plane cycle (from A to B) buckling commenced and was well established at point B. The wall was unloaded after this initial buckling and loaded in the reverse direction (from C to D). Although the wall could survive the maximum out-of-plane drift of 1.5% in both directions and maximum in-plane drift of 1.5% in one direction, it actually collapsed due to out-of-plane buckling during the course of unloading at point H.

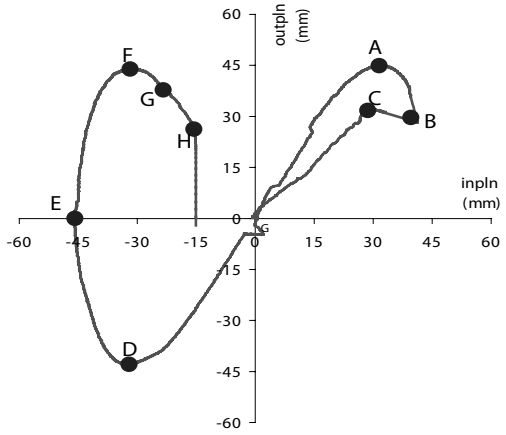

(a) Out-of-plane verses in-plane displacement plot

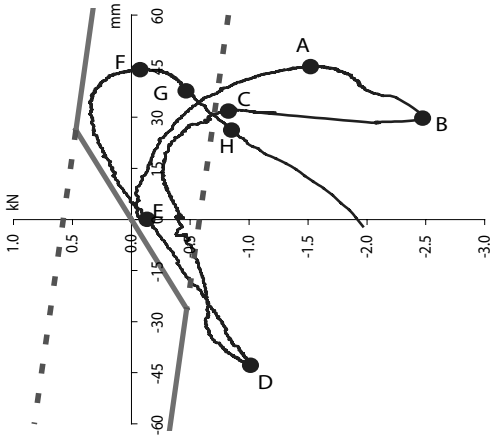

(b) Lateral force verses displacement (out-of-plane)

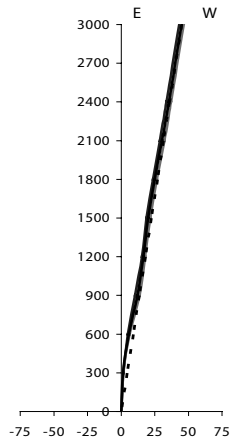

(d) At maximum out-of-plane displacement (point A)

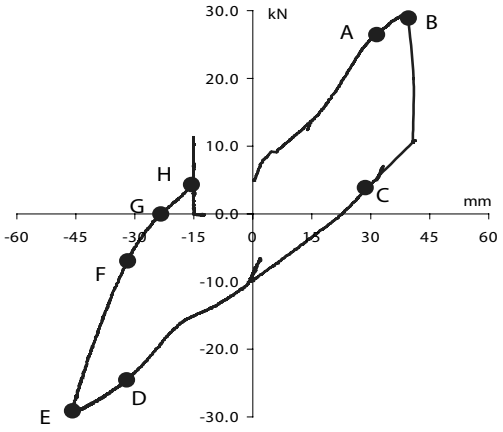

(c) Lateral force verses displacement (in-plane)

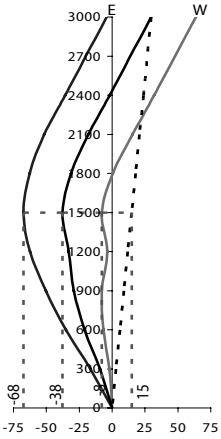

(e) At initial buckling (point B)

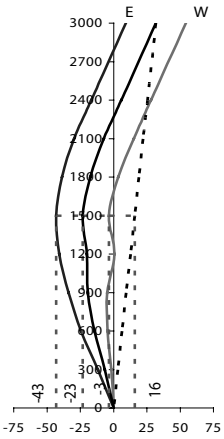

(f) Just after initial buckling (point C)

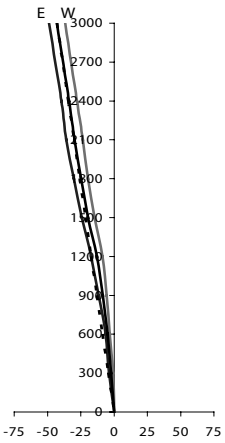

(g) At maximum out-of-plane drift in pull direction (point D)

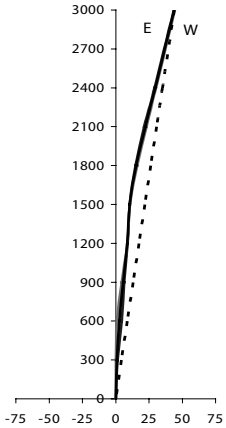

(h) At maximum out-of-plane drift in push direction (point F)

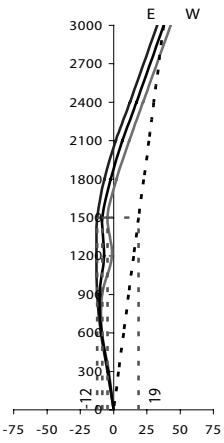

(i) At in-plane unloaded position prior to failure (point G)

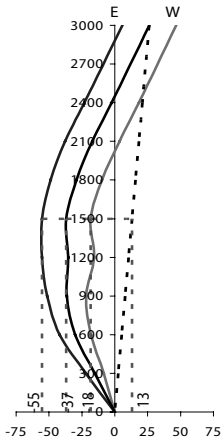

(j) Just prior to failure (point H)

Figure 13: Cyclic response prior to failure for Specimen 1

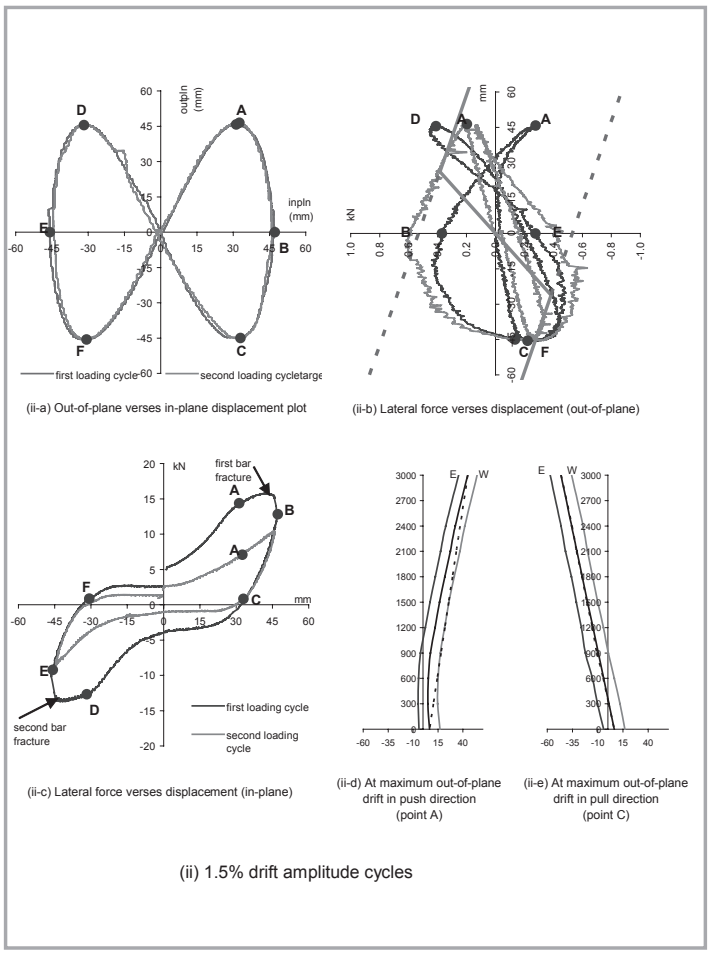

Figure 14: Cyclic response prior to failure for specimen 2

Specimen 2 failure occurred in two ways. The precast wet joint failed first with both the grout layer and wall concrete cracking in compression. Significant concrete spalling was observed during the 1.0% drift cycles. Subsequently, the compression failure of the connection led the wall to crack on its base during the 1.5% and 2.0% drift cycles. Consequently, the exposed longitudinal rebars buckled during compression cycles and fractured in the following tension cycle. The outermost rebars at both ends of the wall were fractured during the first cycle to 1.5% drift, just prior to points B and E on the plots in Figure 14.

7.0 CONCLUSIONS

Both of the specimens were tested until failure modes. Specimen 1 with a moderately high reinforcement ratio of 1.27% failed in lateral torsional buckling mechanism and the failure is sudden. Specimen 1 exhibited a limited ductility of 3. Specimen 2 with a low reinforcement ratio of 0.54% failed in low cycle fatigue behaviour associated with the compression failure of wall concrete and the grout at base joint. Specimen 2 exhibited a ductility of 4. The biaxial loading of wall though not likely to affect the failure mode but significantly reduces the ductility of the wall and brings the wall to a quicker failure than under in-plane loading condition.

Although the wall maximum height to thickness ratio is limited to 30:1 in prescriptive provisions of present design codes BS 8110 [1], NZS 3101 [2] and ACI 318 [3], walls with height to thickness ratio of 60 can be stable even under biaxial loading conditions provided that an excessive longitudinal reinforcement is not present. It is recommended that the wall with ratio of 60:1 may be used for structures requiring limited ductility only; the longitudinal steel volume should be limited to 1%. ■

REFERENCES

[1] British Standard. "Structural of Concrete – Part 1 : Code of Practice for Design and Construction." BS8110-1:1997, London, UK, pp 172, 1997.

[2] NZS 3101: Part: 1: 1995, Concrete Structures Standard, Part 1- "The Design of Concrete Structures", Standards New Zealand, Wellington.

[3] ACI 318-05, "Building Code Requirements for Structural Concrete", American Concrete Institution, ACI Committee 318, New York, U.S.A, pp 430, 2005.

[4] Hamid, N.H. and Surdano, I.,"Dynamic Response of Slender/ Thin Reinforced Precast Concrete Walls using Shaking Table", IEM Journal, The Journal of The Institution of Engineers, Malaysia, Vol. 67, No. 3, pp 18-25, September 2006.

[5] Sudarno, I., (2003). "Performance of Thin Precast Concrete Wall Panels under Dynamic Loading", ME Report, Department of Civil Engineering, University of Canterbury, Christchurch, New Zealand.

[6] Estevez, A. "Biaxial Lateral Load Resistance of a Wall Type Bridge Pier", M.Sc. Report, Faculty of the Graduate School, State University of New York at Buffalo, New York, USA, 1994.

[7] Hamid, N.H.A. "Seismic Damage of Warehouse Buildings Constructed using Precast Hollow Core Panels", PhD Thesis, University of Canterbury, Christchurch, New Zealand, 2006.

PROFILE

ENGR. DR NOR HAYATI BINTI ABDUL HAMID

Engr. Dr Nor Hayati binti Abdul Hamid has been a lecturer at University Teknologi MARA, Shah Alam, Selangor for 15 years. She completed her PhD (Earthquake Engineering) from University of Canterbury, Christchurch, New Zealand in 2006. She received her Master of Science in Construction Management and Structural Engineering from University of NewCastle Upon Tyne, United Kingdom in 1993 and obtained her BSc (Civil Engineering) from University of Pittsburgh, United States of America in 1989. Her research interests are seismic performance of precast buildings under earthquake excitation, dynamic response of thin/ slender wall, design of rocking precast hollow core walls under earthquake, cyclic behaviour of precast hollow core slabs, the interaction of beam-column joints under ground shaking, fragility curves and Incremental Dynamic Analysis (IDA).